EJN European Journal of Neuroscience

FENS Federation of European Neuroscience Societies

European Journal of Neuroscience, pp. 1–11, 2014 doi:10.1111/ejn.12650

Melanocortin 4 receptor activation inhibits presynaptic N-type calcium channels in amygdaloid complex neurons

Francina Agosti,[1] Eduardo J. López Soto,[1] Agustina Cabral,[2] Daniel Castrogiovanni,[3] Helgi B. Schioth,[4] Mario Perelló[2] and Jesica Raingo[1]

[1]Laboratory of Electrophysiology, Multidisciplinary Institute of Cell Biology (IMBICE), Argentine Research Council (CONICET) and Scientific Research Commission, Province of Buenos Aires (CIC-PBA), La Plata, Buenos Aires, Argentina

[2]Laboratory of Neurophysiology, Multidisciplinary Institute of Cell Biology (IMBICE), Argentine Research Council (CONICET) and Scientific Research Commission, Province of Buenos Aires (CIC-PBA), La Plata, Buenos Aires, Argentina

[3]Cell Culture Facility, Multidisciplinary Institute of Cell Biology (IMBICE), Argentine Research Council (CONICET) and Scientific Research Commission, Province of Buenos Aires (CIC-PBA), La Plata, Buenos Aires, Argentina

[4]Department of Neuroscience, Uppsala University, Uppsala, Sweden

Keywords: amygdala, calcium channels, melanocortin receptor, mouse

Abstract

The melanocortin 4 receptor (MC4R) is a G protein-coupled receptor involved in food intake and energy expenditure regulation. MC4R activation modifies neuronal activity but the molecular mechanisms by which this regulation occurs remain unclear. Here, we tested the hypothesis that MC4R activation regulates the activity of voltage-gated calcium channels and, as a consequence, synaptic activity. We also tested whether the proposed effect occurs in the amygdala, a brain area known to mediate the anorexigenic actions of MC4R signaling. Using the patch-clamp technique, we found that the activation of MC4R with its agonist melanotan II specifically inhibited 34.5 ± 1.5% of N-type calcium currents in transiently transfected HEK293 cells. This inhibition was concentration-dependent, voltage-independent and occluded by the $G\alpha_s$ pathway inhibitor cholera toxin. Moreover, we found that melanotan II specifically inhibited 25.9 ± 2.0% of native N-type calcium currents and 55.4 ± 14.4% of evoked inhibitory postsynaptic currents in mouse cultured amygdala neurons. *In vivo*, we found that the MC4R agonist RO27-3225 increased the marker of cellular activity c-Fos in several components of the amygdala, whereas the N-type channel blocker ω conotoxin GVIA increased c-Fos expression exclusively in the central subdivision of the amygdala. Thus, MC4R specifically inhibited the presynaptic N-type channel subtype, and this inhibition may be important for the effects of melanocortin in the central subdivision of the amygdala.

Introduction

In the last few decades, the obesity epidemic has become a major health problem worldwide. Studies looking for effective weight-loss medications have pointed to the melanocortin 4 receptor (MC4R) as a key antiobesity target. MC4R is a G protein-coupled receptor expressed in brain neuronal centers regulating food intake, energy expenditure and autonomic function (Mountjoy *et al.*, 1994; Kishi *et al.*, 2003; Schioth, 2006). MC4R mediates the agonist signal provided by the pro-opiomelanocortin-derived peptide α-melanocyte-stimulating hormone, and the antagonist signal provided by the agouti-related peptide (Cone, 2005). It is known that pharmacological manipulations of MC4R activity strongly affect energy balance. In particular, the selective MC4R agonist decreases, whereas the MC4R antagonist increases food intake and body weight (Fan *et al.*, 1997; Thiele *et al.*, 1998; Hagan *et al.*, 1999; Benoit *et al.*, 2000; Fehm *et al.*, 2001). The neuronal circuits involving MC4R signaling are the best-characterised pathways involved in the regulation of energy homeostasis (Cone, 2005). Interestingly, MC4R regulation of body weight is mediated via divergent neuronal circuits as MC4R in the hypothalamic paraventricular nucleus (PVN) and/or amygdala controls food intake, whereas MC4R in other brain regions controls energy expenditure (Balthasar *et al.*, 2005).

Despite the well-established role of MC4R in the regulation of food intake, the molecular mechanisms by which this receptor regulates neuronal activity remain unclear. MC4R signals through G_s proteins and activates adenylyl cyclase to increase intracellular cAMP with subsequent activation of protein kinase A (Gantz *et al.*, 1993; Gao *et al.*, 2003; Shinyama *et al.*, 2003; Tao, 2010). The MC4R-mediated inhibition of appetite probably involves rapid changes of neuronal activity in both the PVN and amygdala. In this regard, it has been shown that MC4R activation causes depolarisation and increase of the firing activity via postsynaptic mechanisms in PVN neurons (Liu *et al.*, 2003; Ghamari-Langroudi *et al.*, 2011). In addition, MC4R is located on synaptic terminals, suggesting that it may also regulate neuronal circuits via presynaptic mechanisms (Cowley *et al.*, 1999; Fu & van den Pol, 2008; Wan *et al.*, 2008). Indeed, MC4R activation in the PVN induces a significant potentiation of

Correspondence: Jesica Raingo PhD, as above.
E-mail: jraingo@imbice.gov.ar

Received 23 December 2013, revised 30 April 2014, accepted 5 May 2014

GABA-mediated inhibitory postsynaptic responses apparently by a presynaptic action (Cowley *et al.*, 1999). Despite the relevance of the amygdala mediating the anorexic effects of MC4R signaling, the mechanisms involved in MC4R-mediated activation of this brain area have been unexplored. In addition, the molecular targets that could mediate the MC4R actions at synaptic level are currently unknown. Some of the main targets of presynaptic G protein-coupled receptors are the voltage-gated calcium channels (VGCCs) (Currie, 2010). It is currently unknown whether MC4R activation impacts on VGCC activity. In this study, we initially used a mammalian expression system to explore whether different VGCC subtypes are sensitive to MC4R activation. As we found a very selective effect of MC4R activation on the presynaptic N-type subtype of VGCCs, we then used a combination of *in vitro* and *in vivo* studies to explore whether MC4R-mediated regulation of N-type channels occurs in neurons of the amygdala and whether this mechanism is relevant for synaptic activity and neuronal activation.

Materials and methods

Clones and transient transfections

The MC4R clone is contained in the L307 plasmid that has an internal ribosome entry site followed by the enhanced green fluorescent protein sequence to identify transfected cells. This plasmid was constructed from a commercial plasmid (cat. no. MMM1013-99829006, no. BC116957, Open Biosystems, Huntsville, AL, USA) with invaluable help from Dr Mikhail Khvotchev (laboratory of Dr Ege Kavalali, UT Southwestern Medical Center). The clones of calcium channels used for this study were a gift from Dr Diane Lipscombe (Brown University): $Ca_V2.2$ (no. AF055477), $Ca_V1.2$ (no. AY728090), $Ca_V1.3$ (no. AF370009), $Ca_V2.1$ (no. AY714490), and the auxiliary subunits $Ca_V\beta_3$ (no. M88751) and $Ca_V\alpha_2\delta_1$ (no. AF286488). In some experiments, regulator G protein signaling 2 (RGS2) contained in a pCI plasmid (Promega, Madison, WI, USA) was used. HEK293 cells were growth at 80% of confluence in Dulbecco's modified Eagle's medium (cat. no. P3030, Microvet, Buenos Aires, Argentina) with 10% fetal bovine serum (cat. no. 1650-01, Internegocios, Mercedes, Buenos Aires, Argentina) and transfected 24 h later with MC4R and the calcium channels with the auxiliary subunits in a 1 : 1 molar ratio by the cationic liposomes method (Lipofectamine 2000, Invitrogen, Carlsbad, CA, USA). After 24 h, cells were dispersed with 0.25 mg/mL trypsin, rinsed twice and kept at room temperature (23 °C) on Dulbecco's modified Eagle's medium during the patch-clamp experimental day.

Drugs

The MC4/MC3 agonist, melanotan II (MTII) (cat. no. 043-23, Phoenix Pharmaceutical, Karlsruhe, Baden-Württemberg, Germany), the inhibitor of G_s protein, cholera toxin (cat. no. C8052, Sigma Aldrich) and the P/Q-type channel blocker, ω agatoxin IVA (cat. no. 4256-s, Peptides International, Louisville, KY, USA) were used for *in vitro* experiments. The MC4R-specific agonist, RO27-3225 (cat. no. R3905, Sigma Aldrich) and the N-type channel blocker, ω conotoxin GVIA (cat. no. C-300, Alomone Labs, Jerusalem, Israel) were used for *in vivo* and *in vitro* experiments.

Animals

The C57BL6/J mice were bred at the animal facility of the Multidisciplinary Institute of Cell Biology (IMBICE). Animals were housed in a 12 h light/dark cycle with regular chow and water available *ad libitum*. This study was carried out in strict accordance with the recommendations in the Guide for the Care and Use of Laboratory Animals of the National Institutes of Health. All experimentation received approval from the Institutional Animal Care and Use Committee of the IMBICE.

Primary amygdaloid neuronal cultures

Neuronal cultures were obtained from mice on embryonic day 16–17. The procedure protocol was similar to that previously described (Raingo *et al.*, 2012). Briefly, pregnant mice were anesthetised with chloral hydrate (500 mg/kg) to remove the embryos. The embryo brains were exposed and placed on the dorsal face to remove the hypothalamus with forceps. Subsequently, brains were transversely sliced with a cut running ~1 mm deep from the ventral surface of the temporal lobe to the midline. The optic chiasm and rostral edge of mammillary bodies were used as the rostral and caudal limits, respectively. The block of tissue obtained contained mainly the amygdaloid complex and neighboring piriform cortex from each hemisphere (Swanson & Petrovich, 1998). Blocks of tissue were placed in Hank's solution, and cells were dissociated with a solution containing trypsin (0.25 mg/mL) (cat. no. L2700-100, Microvet) and deoxyribonuclease I from bovine pancreas (0.28 mg/mL) (cat. no. D5025, Sigma Aldrich) at 37 °C for 20 min, then 300 μL of fetal bovine serum was added to stop the digestion and cells were mechanically dissociated using several glass pipettes with consecutively smaller tip diameters. A total of 50 000 cells were plated on 12 mm diameter glasses previously treated with poly-L-lysine (cat. no. P8920, Sigma Aldrich) and laid over 15 mm diameter wells. Cells were incubated at 37 °C in a 95% O_2 and 5% CO_2 atmosphere with Dulbecco's modified Eagle's medium/F12 (1 : 1) medium supplemented with 10% fetal bovine serum, 0.25% glucose, 2 mM glutamine (cat. no. 21051-016, Gibco, USA), 3.3 μg/mL insulin (Nordisk Pharm Ind., Inc., Clayton, NC, USA), 5 U/mL penicillin G sodium salt (Richet, Buenos Aires, Argentina), 5 μg/mL streptomycin (Richet), 40 μg/mL gentamicin sulfate salt (Richet), 1% vitamin solution (cat. no. L2112-100, Microvet) and B27 supplement (1 : 50) (cat. no. 17504-044, Gibco). On the fourth day in culture, half of the incubation medium was replaced with medium containing cytosine β-D-arabinofuranoside to reach a final concentration of 5 μM (cat. no. C1768, Sigma Aldrich). The cultures enriched in amygdaloid complex neurons were cultured for 6–22 days and used to perform patch-clamp experiments.

Electrophysiology

Ionic currents were recorded with an Axopatch 200 amplifier (Molecular Devices). Data were sampled at 20 kHz and filtered at 10 kHz (−3 dB) using pclamp8.2 software. Series resistances of less than 6 MΩ were admitted and compensated 80% with a 10 μs lag time. Recording electrodes had resistances of 2–4 MΩ when filled with the internal solution. Current leak was subtracted on-line using a P/-4 protocol. All recordings were obtained at room temperature.

Calcium currents in transiently transfected HEK293 cells

Whole-cell patch-clamp recordings were performed on transfected (enhanced green fluorescent protein-positive) HEK293 cells. The internal pipette solution contained (in mM): 134 CsCl, 10 EGTA, 1 EDTA, 10 HEPES and 4 MgATP (pH 7.2 with CsOH). The external solution contained (in mM): 2 $CaCl_2$, 1 $MgCl_2$, 10 HEPES and 140 choline chloride (pH 7.4 with CsOH). Cells were typically held at

−100 mV to remove closed-state inactivation (Thaler *et al.*, 2004). The test-pulse protocol was square pulses applied from −100 to 10 mV for 15 ms every 10 s. The prepulse protocol was a prepulse of 15 ms at +80 mV applied at 12 ms before the test pulse to remove the voltage-dependent inhibition of VGCCs (Ikeda & Dunlap, 1999). The application of the +80 mV prepulse failed to modify calcium currents in control (I_{pp} = −0.95 ± 1.67% of I control, n = 5, P = 0.6). The current–voltage relationship protocol was 5 mV increasing square test pulses of 15 ms duration applied from −60 to +80 mV (Raingo *et al.*, 2007).

Barium currents in primary neuronal cultures

At 6–10 days *in vitro*, neurons were patch-clamped with the same internal solution as described for HEK293 cells in whole-cell mode. Sodium currents were measured with a high-sodium external solution containing (in mM): 135 NaCl, 4.7 KCl, 1.2 $MgCl_2$, 2.5 $CaCl_2$, 10 HEPES and 10 glucose (pH 7.4 with NaOH). After neurons were clamped at negative potentials, the external solution was replaced by a high-barium solution to measure VGCC currents. The high-barium solution contained (in mM): 1 $MgCl_2$, 10 HEPES, 10 glucose, 10 $BaCl_2$, 20 tetraethyl-ammonium chloride, 110 choline chloride and 0.001 tetrodotoxin (Sigma Aldrich) (pH 7.4 with CsOH). Neurons were held at −80 mV, and test pulses to 0 mV were applied for 20 ms every 10 s.

Postsynaptic currents in primary neuronal cultures

At 13–22 days *in vitro*, neurons were patch-clamped with an internal solution containing (in mM): 115 Cs-methanesulfonate, 10 CsCl, 5 NaCl, 10 HEPES, 20 tetraethylammonium, 4 Mg-ATP, 0.3 Na-GTP, 0.6 EGTA and 10 lidocaine *N*-ethyl bromide (QX314). We used the high-sodium external solution described in the previous paragraph, containing 10 μM 6-cyano-7-nitroquinoxaline-2,3-dione (Alomone Labs) to isolate inhibitory postsynaptic currents (IPSCs) or 50 μM picrotoxin (Sigma Aldrich) to isolate excitatory postsynaptic currents. Neurons were held at −80 mV and, to elicit evoked responses, electrical stimulation was delivered through parallel platinum electrodes (duration, 1 ms; amplitude, 20 mA). Spontaneous miniature IPSCs (mIPSCs) were recorded with the addition of 1 μM tetrodotoxin (Raingo *et al.*, 2012).

Animal treatments and stereotaxic surgeries

Experiments were performed with adult (2–3-month-old) male mice, which were stereotaxically implanted with a single indwelling sterile guide cannula (4 mm long, 22 gauge, Plastics One) into the lateral ventricle [intracerebroventricular (ICV)]. The placement coordinates for the lateral ventricle were: AP, −0.34 mm; L, +1 mm and V, −2.3 mm. A 28-gauge obturator was inserted into each cannula. For these ICV surgeries, mice were anesthetised with ketamine (10 mg/kg) and xylazine (1 mg/kg). After surgery, animals were individually housed and allowed to recover for at least 5 days. Mice were accustomed to handling by removal of the dummy cannula and connection to an empty cannula connector daily for at least 4 days prior to experimentation, to reduce stress. Correct placement of the cannula was confirmed by histological observation at the end of the experiment. On the morning of the experimental day, animals were ICV injected with 4 μL of vehicle (artificial cerebrospinal fluid) either alone or containing the specific MC4R agonist RO27-3225 (4 μg/mouse), or the specific N-type calcium channel blocker ω conotoxin GVIA (0.1 μg/mouse). All ICV injections were made over 2 min through a 30 gauge needle that extended 0.5 mm below the guide cannula and was connected by polyethylene tubing to a 5 μL Hamilton syringe. The needle was left in place for 2 min following the injection to prevent backflow of the injected solution. After 2 h, mice were anesthetised with chloral hydrate (500 mg/kg) and perfused with formalin as previously described (Cabral *et al.*, 2012).

Assessment of c-Fos localisation by immunohistochemistry

The brains of perfused mice were removed, postfixed, immersed in 20% sucrose and cut coronally at 20 μm into three equal series on a sliding cryostat as previously described (Cabral *et al.*, 2012). The c-Fos immunostaining was performed as described previously (Cabral *et al.*, 2012). Briefly, sections were pretreated with 1% H_2O_2, treated with blocking solution (3% normal donkey serum and 0.25% TritonX in phosphate-buffered saline), and incubated with anti-c-Fos antibody (1 : 15 000, cat. no. PC38, Calbiochem/Oncogene, Darmstadt, Hesse, Germany) for 2 days at 4 °C. The sections were then treated with biotinylated donkey anti-rabbit antibody (1 : 1000, Jackson Immuno Research Laboratories, West Grove, PA, USA) for 1 h, and with Vectastain Elite ABC kit (Vector Laboratories, Burlingame, CA, USA) for 1 h, according to the manufacturer's protocols. The visible signal was then developed with 3-3′-diaminobenzidine/nickel solution, giving a black/purple precipitate. Sections were sequentially mounted on glass slides, and cover slipped with mounting media. Results were visualised using bright-field light sources. Bright-field images were acquired with a Nikon Eclipse 50i and a DS-Ri1 Nikon digital camera. An image-editing software program, ADOBE PHOTOSHOP CS2, was used to adjust contrast and brightness. Quantitative analysis was performed in three animals per condition.

Quantitative analysis of immunohistochemical data

For the analysis, the amygdaloid complex was subdivided as previously suggested by Sah *et al.* (2003). The amygdaloid complex divisions included: (i) the basolateral subdivision, which included the basolateral amygdala (BLA), basomedial amygdala, and accessory basal nucleus; (ii) the cortical-like subdivision, which included the cortical nuclei and nucleus of the lateral olfactory tract; and (iii) the centro-medial subdivision composed of the medial amygdala and central amygdala (CeA). Neuroanatomical limits were defined as described in the mouse brain atlas of Paxinos & Franklin (2001). The total number of c-Fos-immunoreactive (IR) cells was quantified in the BLA and CeA of the amygdaloid complex. For this purpose, cells containing distinct nuclear black/purple precipitate were quantified in one out of three complete series of coronal sections. These numbers were then summed and multiplied by three. The total c-Fos-IR cells of each amygdaloid subdivision were estimated in sections between bregma −0.70 and −1.94 mm. All analyses were carried out in similar areas under the same optical and light conditions. Data are expressed as total c-Fos-IR cells per amygdaloid division per side.

Statistics

Data are expressed as mean ± SE. Normal distribution was tested with D'Agostino–Pearson and Shapiro–Wik tests (GRAPHPAD PRISM 5 software). Data with a normal distribution were analysed with one- or two-sample Student's *t*-tests (OriginPro8). Data without a Gaussian distribution were analysed with non-parametric tests, i.e. Wilcoxon signed-rank test (equivalent to one-sample Student's

t-test) and Mann–Whitney test (equivalent to two-sample Student's *t*-test) (GRAPHPAD PRISM 5 software). Concentration–response curves were fitted with the Hill equation and current–voltage curves with a Boltzmann lineal equation (OriginPro 8). The number of c-Fos-IR cells per amygdaloid complex subdivision was analysed by a one-way ANOVA test followed by the Newman–Keuls test (GRAPHPAD PRISM 5 software). Significant differences were considered when $P < 0.05$.

Results

Agonist-induced melanocortin 4 receptor activation inhibits N-type calcium channels by a G_s-mediated voltage-independent mechanism

In order to test the effect of MC4R activation on VGCCs, we exposed HEK293 cells co-expressing MC4R with different VGCC subtypes and the auxiliary subunits ($Ca_V\beta_3$ and $Ca_V\alpha_2\delta_1$) to the MC3/4R agonist MTII. We found no effect of MTII on cells co-expressing MC4R and L-type ($Ca_V1.2$ and $Ca_V1.3$) or P/Q-type ($Ca_V2.1$) channels, whereas MTII application rapidly inhibited N-type calcium channels ($Ca_V2.2$) (Fig. 1A). The inhibition of $Ca_V2.2$ by MC4R activation was concentration-dependent and had a median effective concentration (EC_{50}) of 28.4 ± 1.2 nM (Fig. 1B). As a control, we tested MTII in cells expressing $Ca_V2.2$ channels without MC4R and failed to observe an effect (1.50 ± 1.7%, $n = 5$, not significantly different from zero, $P = 0.4$). Thus, we concluded that the agonist-induced MC4R activation specifically inhibited the $Ca_V2.2$ subtype of VGCCs.

We next tested the mechanism by which MC4R regulates $Ca_V2.2$ activity. We first assayed the voltage dependency of MC4R-mediated $Ca_V2.2$ inhibition by current–voltage curves in control conditions and after bath application of 250 nM MTII. We found that the half-maximal activation voltages ($V_{1/2}$) were equal in both conditions (control, −1.28 ± 1.3 mV; MTII, 0.12 ± 3.0 mV, $n = 7$, $P = 0.56$), indicating that MC4R-mediated $Ca_V2.2$ inhibition was independent of the voltage applied (Fig. 2A). To confirm our result, we assayed the effect of a + 80 mV prepulse on the MC4R activity-mediated inhibition of $Ca_V2.2$ currents evoked by a + 10 mV pulse. This maneuver is commonly used to remove the voltage-dependent inhibition by G proteins. We found that the prepulse failed to modify the percentage of inhibition (Fig. 2B); thus, the MC4R-mediated $Ca_V2.2$ inhibition involved a voltage-independent mechanism. As the voltage-independent inhibition of VGCCs is mostly mediated by the Gα subunit of G proteins, we tested the effect of RGS2, a GTPase that occludes the activity of several Gα protein subtypes (Heximer *et al.*, 1997; Ingi *et al.*, 1998; Han *et al.*, 2006; Roy *et al.*, 2006a,b). In HEK293 cells co-transfected with RGS2, MC4R, $Ca_V2.2$ and the auxiliary subunits, we found that RGS2 expression reduced the MC4R-mediated $Ca_V2.2$ current inhibition (Fig. 2C). As MC4R couples mainly to G_s, we next investigated whether the MC4R-mediated inhibition of $Ca_V2.2$ was observed in the presence of cholera toxin, which specifically prevents G_s hydrolyzing GTP. We found that MTII failed to inhibit $Ca_V2.2$ currents in the presence

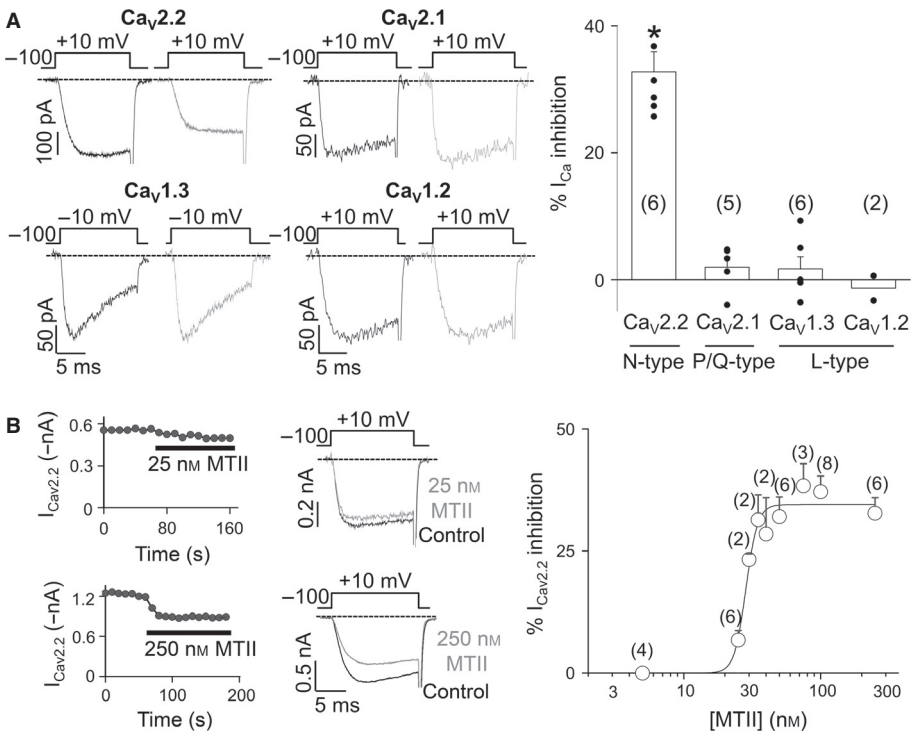

FIG. 1. Effect of MC4R activation on different subtypes of VGCCs and the concentration dependency of $Ca_V2.2$ inhibition induced by MTII. (A) Representative current traces from HEK293 cells co-expressing MC4R and $Ca_V2.2$, $Ca_V2.1$, $Ca_V1.3$ or $Ca_V1.2$ evoked at +10 mV (except for $Ca_V1.3$, evoked at −10 mV) for 15 ms from a holding potential of −100 mV in control conditions (black traces) and after the application of 250 nM MTII (gray traces). Averaged changes in peak current amplitude in response to the application of 250 nM MTII. (B) Left: time courses of peak calcium current (evoked by a 15 ms +10 mV step from a holding potential of −100 mV) inhibition by the application of 25 nM (top) and 250 nM (bottom) MTII. Center: representative calcium current traces from HEK293 cells co-expressing MC4R and $Ca_V2.2$ evoked at +10 mV from a holding potential of −100 mV for 15 ms under control conditions (black) and after the application of 25 nM (gray) (top) and 250 nM (bottom) MTII. Right: MTII concentration–response curve of $Ca_V2.2$ current inhibition in HEK293 cells co-expressing $Ca_V2.2$ and MC4R (MTII concentration range 5–250 nM). Line represents the fitted Hill equation ($r^2 = 0.76$). The estimated MTII EC_{50} is 28.5 ± 1.3 nM, the maximum inhibition is 34.5 ± 1.5% and the Hill coefficient is 10.2 ± 3.7. *Statistically different from zero ($P < 0.05$).

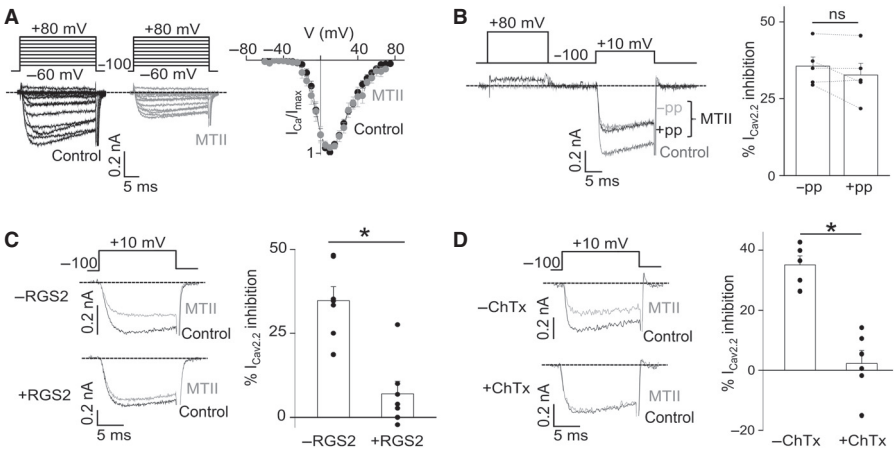

FIG. 2. Mechanism of $Ca_V2.2$ inhibition induced by MC4R activation. (A) Left: representative current traces evoked at increasing potentials by 10 mV for 15 ms in control conditions (black traces) and with the application of 250 nM MTII (gray traces). Right: current (I_{Ca})–voltage (V) curve in control conditions (black) and after the application of 250 nM MTII (gray) ($n = 6$ cells). (B) Left: representative current traces evoked at +10 mV that were preceded (+pp) or not preceded (−pp) by a prepulse at +80 mV in control conditions and in the presence of 250 nM MTII. Right: averaged changes in peak current amplitude in response to the application of 250 nM MTII with (+pp) and without (−pp) prepulse application ($n = 5$ cells). (C) Representative calcium current traces in HEK293 cells co-expressing MC4R and $Ca_V2.2$ (−RGS2), or MC4R, $Ca_V2.2$ and RGS2 (+RGS2), evoked at +10 mV from a holding potential of −100 mV for 15 ms in control conditions (black) and after the application of 250 nM MTII (gray). Bar graph representing the averaged changes in peak current amplitude by the application of MTII in both conditions ($n = 7$ cells for each condition). (D) Representative calcium current traces in HEK293 cells co-expressing MC4R and $Ca_V2.2$ with (+ChTx) or without (−ChTx) preincubation for 20 h with 500 ng/mL cholera toxin evoked by a + 10 mV step from a holding potential of −100 mV for 15 ms in control conditions (black traces) and after the application of MTII (gray traces). Bar graph representing the averaged changes in peak current amplitude in response to the application of MTII in –ChTx ($n = 5$ cells) and +ChTx conditions ($n = 6$ cells). ns, not significantly different. *Statistically different ($P < 0.05$).

of cholera toxin (Fig. 2D). We concluded that MC4R-mediated $Ca_V2.2$ inhibition was mediated by a $G\alpha_s$-dependent signaling cascade and, as a consequence, was completely voltage-independent.

Agonist-induced melanocortin 4 receptor activation inhibits native N-type currents in neurons from the mouse amygdaloid complex

We next explored whether the MC4R-mediated N-type calcium channel inhibition occurred in cultured amygdaloid neurons, which express native levels of both MC4R and channels (Lee *et al.*, 2002; Kishi *et al.*, 2003; Liu *et al.*, 2003; Gelez *et al.*, 2010). Neurons were identified based on the cellular morphology together with the presence of large sodium currents recorded in a high-sodium external solution. The sodium currents were fully sensitive to 1 μM tetrodotoxin in our experimental conditions (Fig. 3A). When the high-sodium solution was replaced by an external solution containing 10 mM $BaCl_2$, we were able to record barium currents through VGCCs that were completely inhibited by 100 μM $CdCl_2$ (Fig. 3A). On this setting, we found that MTII had a concentration-dependent inhibitory effect on barium currents. A saturating concentration of MTII (250 nM) inhibited VGCC currents in 15 out of 17 tested neurons. We fitted the concentration-inhibition data with a Hill equation, obtaining an EC_{50} of 18.0 ± 3.7 nM (Fig. 3B). As MTII also stimulates MC3R activity, we tested the effect of a saturating concentration of the MC4R-specific agonist RO27-3225 (250 nM) (Benoit *et al.*, 2000), and found that 250 nM RO27-3225 had an equivalent effect to 250 nM MTII (Fig. 3B). In order to evaluate to what extent the MC4R-induced barium current inhibition was mediated by N-type or P/Q-type calcium channels, we used saturating concentrations of the N-type calcium channel blocker ω conotoxin GVIA or the P/Q-type calcium channel blocker ω agatoxin IVA. We found that 1 μM ω conotoxin GVIA inhibited 41.7 ± 13.9% of the total barium current (Fig. 3C). In the presence of ω conotoxin GVIA, MTII had no further inhibitory effect on the total barium currents (Fig. 3C). Inversely, the inhibitory effect of ω conotoxin GVIA on the total barium currents was reduced to half when MTII was present (Fig. 3C), as expected if the MTII-induced inhibition of barium currents is specific and corresponds to around 40% of the total N-type currents (as observed in transfected HEK293 cells). However, we found that 0.2 μM ω agatoxin IVA inhibited only 12.8 ± 2.3% ($n = 5$, $P = 0.005$) of the total current, and that the inhibitory effect of MTII on the total barium currents was unaffected by the presence of this P/Q-type channel blocker (Fig. 3D). Thus, our results demonstrated that N-type calcium channels were sensitive to MC4R activation, whereas P/Q-type currents were not affected by this receptor. Thereby, we recapitulated in amygdalar neurons our previous findings in transfected HEK293 cells.

Melanocortin 4 receptor activation reduces N-type calcium channel-dependent GABAergic neurotransmission in amygdaloid complex primary neuronal cultures

The MC4R activation stimulated neuronal activity in the amygdaloid complex (Thiele *et al.*, 1998; Benoit *et al.*, 2000). As we found that MC4R activation inhibits N-type currents in amygdalar neurons in culture, we hypothesised that inhibition of N-type channels occurs at GABAergic terminals, contributing to the overall stimulatory effect of the MC4R agonist in this brain region. Thus, we tested whether the MC4R-mediated N-type channel inhibition is relevant for the synaptic activity in embryonic amygdaloid complex neuronal cultures. We first characterised the contribution of N-type or P/Q-type channels to triggering neurotransmitter release in mature amygdaloid complex cultures (from 15 to 22 days *in vitro*) by assaying the effect of specific blockers (ω conotoxin GVIA or ω agatoxin IVA, respectively) on IPSCs. We found that ω conotoxin GVIA inhibited the IPSC peak size to a larger extent than ω agatoxin IVA (71.4 ± 9.1% vs. 39.2 ± 6.4%, $P < 0.05$, Fig. 4A and B).

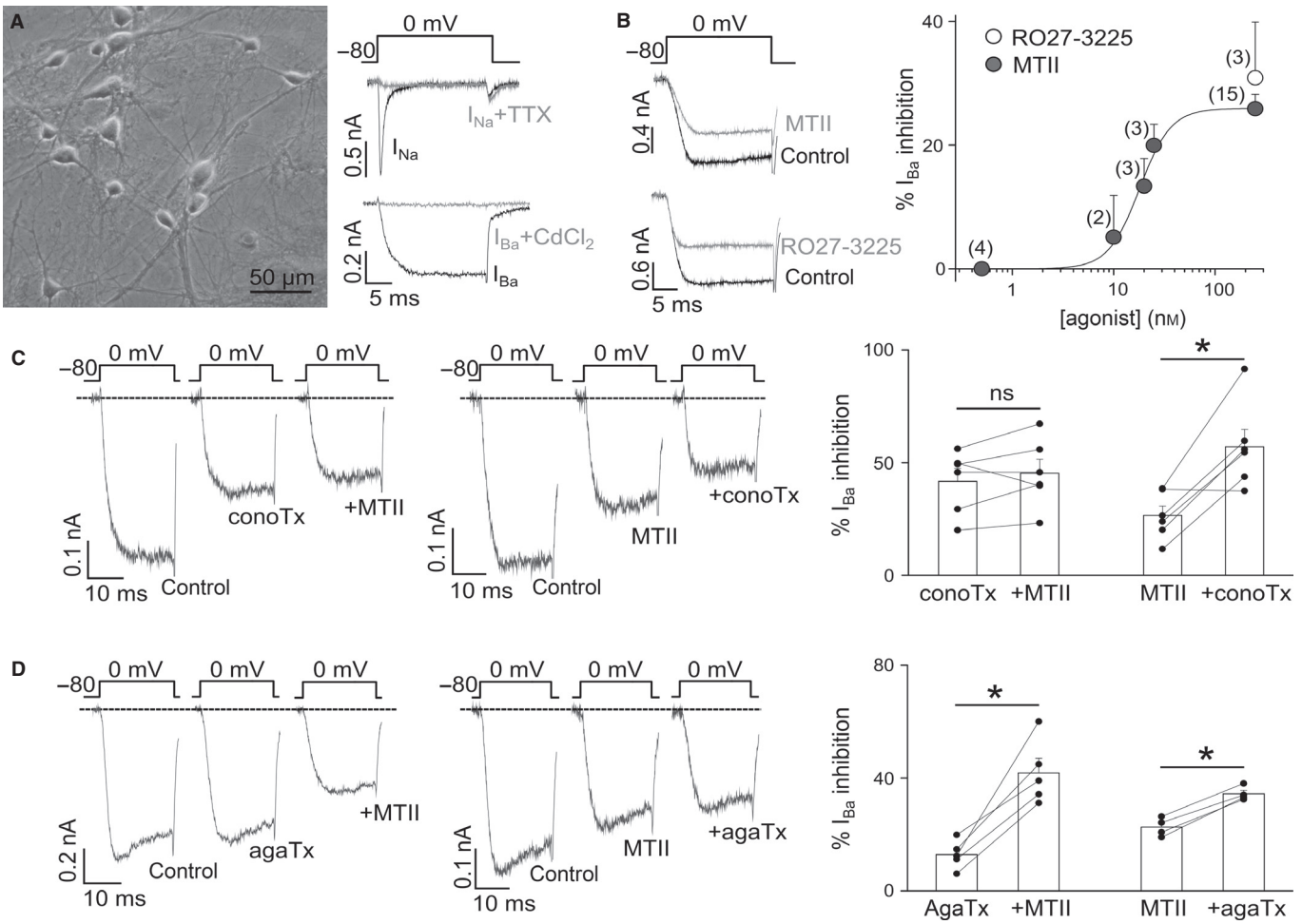

FIG. 3. N-type current inhibition induced by MC4R activation in cultured amygdaloid complex neurons. (A) Microphotograph of a 10 day *in vitro* amygdaloid neuronal culture and representative traces of currents evoked by a step to 0 mV from a holding potential of −80 mV for 20 ms with sodium (I_{Na}) and barium (I_{Ba}) as permeable ions with or without the application of blockers [1 µM tetrodotoxin (TTX) for I_{Na} and 100 µM $CdCl_2$ for I_{Ba}]. (B) Representative barium current traces from cultured neurons evoked at 0 mV from a holding potential of −80 mV for 20 ms in control conditions and with the application of 250 nM MTII (top) and 250 nM RO27-3225 (bottom), and averaged percent of barium current inhibition vs. RO27-3225 and MTII concentrations. The fitted curve was obtained with a Hill equation ($r^2 = 0.62$). The EC_{50} for MTII is 18.0 ± 3.7 nM, the maximum inhibition is 25.9 ± 2.0% and the Hill coefficient is 2.8 ± 1.9. (C) Representative current traces from cultured amygdaloid neurons evoked by a 0 mV step from −80 mV for 20 ms in control conditions and after the application of 1 µM ω conotoxin GVIA (conoTx) and/or 250 nM MTII. Bars represent averaged peak barium current changes by conoTx (conoTx) and conoTx plus MTII (+MTII), and by MTII (MTII) and MTII plus conoTx (+conoTx) ($n = 6$ neurons each). (D) Representative current traces from cultured amygdaloid neurons evoked by a 0 mV step from −80 mV for 20 ms in control conditions and after the application of 0.2 µM ω agatoxin IVA (agaTx) and/or 250 nM MTII. Bars represent averaged peak barium current changes by agaTx (agaTx) and agaTx plus MTII (+MTII), and by MTII (MTII) and MTII plus agaTx (+agaTx) ($n = 4$ and $n = 3$ neurons, respectively). ns, not significantly different. *Statistically different ($P < 0.05$).

Moreover, the application of both toxins almost fully inhibited the total GABAergic evoked IPSCs (93.23 ± 3.43%, $n = 3$, not significantly different from 100%, $P = 0.19$). Our data indicated that N-type calcium channels had more control of GABAergic neurotransmission than P/Q-type channels in our recording conditions.

We next investigated whether MC4R activation modulates neurotransmitter release in amygdaloid complex neuronal cultures. We found that MTII inhibited IPSC peak size by 55.4 ± 14.4% (Fig. 5A). We then tested whether MTII affected GABA release stimulated by a hyperosmotic solution, which was independent of calcium influx through VGCCs (Raingo *et al.*, 2012). We found that MTII failed to change GABAergic transmission stimulated by a hyperosmotic sucrose solution (0.5 M, Fig. 5B). Moreover, we recorded mIPSCs and found that MTII did not modify the frequency but slightly increased the mIPSC size (Fig. 5C). We also evaluated the effect of MTII on glutamatergic neurotransmission, and found that MTII failed to modify excitatory postsynaptic currents (−17.8 ± 14.4%, $n = 5$, $P = 0.3$). Thus, we found that MC4R activation inhibited N-type calcium channel-evoked GABAergic neurotransmission in embryonic cultures, whereas it failed to modify VGCC-independent GABA release or the excitatory postsynaptic currents. Moreover, the effect of MTII on IPSCs overcame a mild postsynaptic stimulatory effect on mIPSC size. Thus, our results suggested that MC4R activity reduced GABAergic neurotransmission by inhibiting presynaptic N-type calcium currents.

Blockade of N-type channels mimics the increase of c-Fos expression induced by a melanocortin 4 receptor agonist exclusively in the central amygdaloid nucleus of the amygdaloid complex

Next we hypothesised that the MC4R-mediated reduction of GABAergic tone could mediate the previously described MC4R-dependent transcriptional activation of amygdala neurons (Benoit

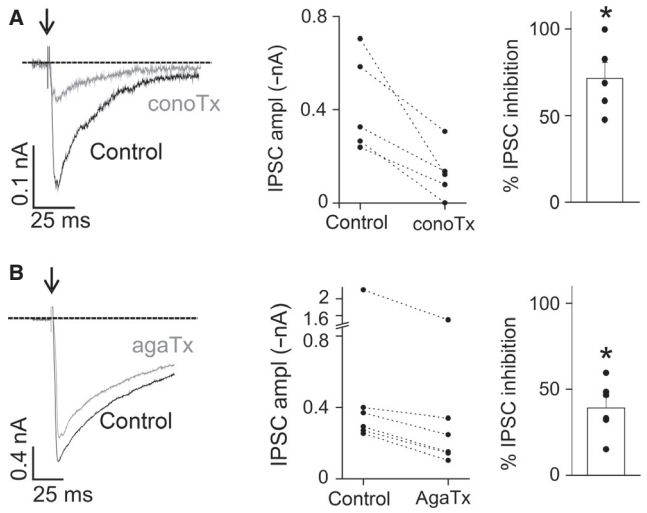

FIG. 4. GABAergic neurotransmission in amygdaloid complex cultures is mostly controlled by N-type calcium channels. (A) Left: representative traces of evoked IPSCs (registered at −80 mV) in amygdalar cultured neurons in control conditions and after the application of 3 μM ω conotoxin GVIA (conoTx). Center: amplitude changes on IPSC peaks before and after the application of 3 μM conoTx. Right: average percent for IPSC amplitude inhibition after the application of 3 μM conoTx (n = 5 neurons). (B) Left: representative traces of evoked IPSCs in amygdaloid cultured neurons in control conditions and after the application of 0.2 μM ω agatoxin IVA (agaTx). Center: amplitude changes on IPSC peaks before and after the application of 0.2 μM agaTx. Right: average percent for IPSC amplitude inhibition after the application of 0.2 μM agaTx (n = 6 neurons). *Statistically different from zero ($P < 0.05$).

et al., 2000). Thus, we performed *in vivo* experiments to compare the induction of the marker of neuronal activation c-Fos in the amygdaloid complex of mice that were treated ICV with the MC4R agonist RO27-3225 or with the N-type calcium channel blocker ω conotoxin GVIA. We found that RO27-3225 induced a profound increase of the number of c-Fos-IR cells in the CeA and BLA of the amygdaloid complex in comparison with the numbers observed in vehicle-treated mice (Fig. 6). In contrast, we found that ω conotoxin GVIA induced an increase in the number of c-Fos-IR cells exclusively in the CeA subdivision of the amygdaloid complex. Thus, blockade of N-type channels mimicked the pattern of c-Fos expression induced by an MC4R agonist only in the CeA, where GABAergic innervations are particularly profuse (Sun & Cassell, 1993; Thiele *et al.*, 1998; Benoit *et al.*, 2000; Pare *et al.*, 2004; Jovanovic & Ressler, 2010).

Discussion

The current study provides the first characterisation of the MC4R-mediated regulation of VGCCs and proposes the CeA of the amygdaloid complex as a relevant brain area for the MC4R-induced inhibition of N-type calcium channels. Our results indicate that the agonist-induced MC4R activation specifically inhibits N-type channels and fails to affect P/Q-type and L-type channels. We recapitulated this specificity in cultured amygdala neurons, where the MC4R agonist has no effect in the presence of saturating concentrations of the N-type calcium channel blocker (ω conotoxin GVIA). This observation is in agreement with previous data showing that N-type channels are the VGCC subtype that is most sensitive to inhibition via activation of different G protein-mediated pathways (Tedford & Zamponi, 2006). Our results suggest that MC4R will affect VGCC currents only at presynaptic terminals, where N-type and P/Q-type calcium channels are enriched and control synaptic vesicles release (Maximov *et al.*, 1999; Missler *et al.*, 2003). Moreover, this MC4R-mediated effect will be limited to synapses where N-type channels

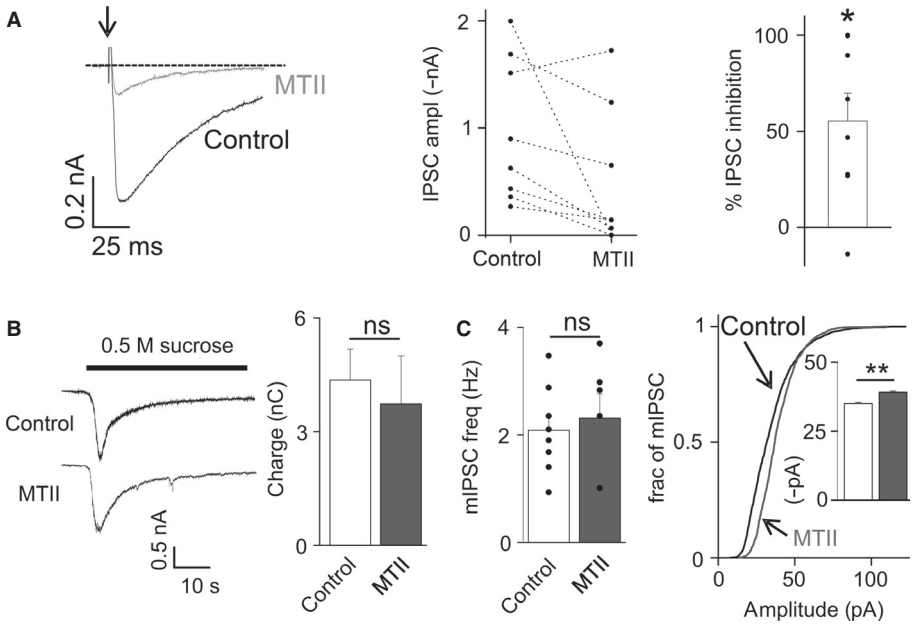

FIG. 5. MC4R activation inhibits VGCC-dependent GABAergic neurotransmission in amygdaloid complex cultures. (A) Left: representative traces of evoked IPSCs (registered at −80 mV) in amygdaloid cultured neurons in control conditions and after the application of 250 nM MTII. Center: amplitude changes on IPSC peaks before and after the application of 250 nM MTII. Right: average percent for IPSC amplitude inhibition after the application of 250 nM MTII (n = 8 neurons). (B) Representative traces (left) and average charge transfer values (right) integrated during the first 3 s before and 3 s after hypertonic stimulation (0.5 M sucrose) in cultured amygdaloid neurons registered at −80 mV (n = 5 neurons each experiment). (C) Left: average frequency of mIPSCs in control conditions and after the application of 250 nM MTII (control, n = 9; MTII, n = 6 neuron). Right: amplitude distribution and average amplitude of mIPSCs in control conditions and after the application of 250 nM MTII. *Statistically different from zero ($P < 0.05$). ns, not significantly different. **Statistically different ($P < 0.05$).

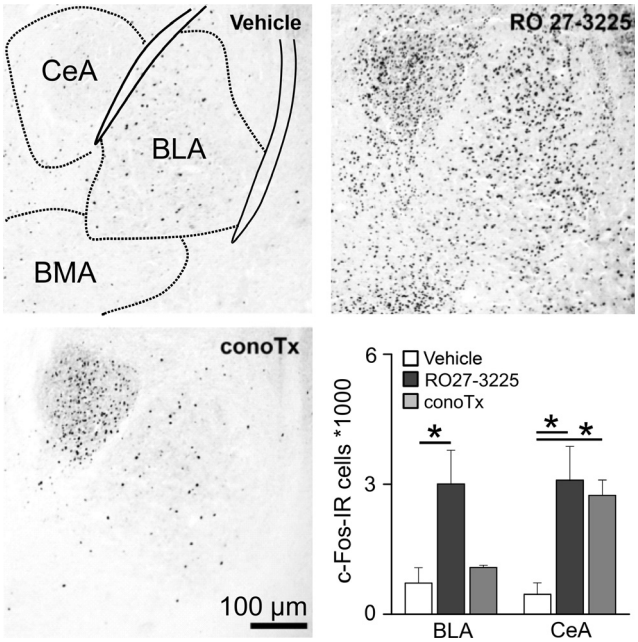

FIG. 6. c-Fos staining in specific subregions of the amygdala. Representative microphotographs of c-Fos (black/purple signal) immunostaining in the amygdala of RO27-3225-treated (left, top), ω conotoxin GVIA (conoTx)-treated (right, top) and vehicle-treated (left, bottom) groups with a schematic diagram of amygdala subregions and known GABAergic connections in a coronal section of the mouse brain. BMA, basomedial amygdala. Drawn neurons in gray represent GABAergic connections. Right, bottom: quantitative analysis of c-Fos staining in BLA and CeA subregions of the amygdala. *Significantly different from vehicle group ($P < 0.05$).

contribute to calcium influx. However, the fact that we found no effect of MC4R activation on VGCCs enriched at the soma and dendrites (L-type calcium channels) agrees with a previous report showing that MC4R activation at neuronal soma increases cytosolic calcium levels from intracellular compartments without contributions from external calcium influx (Newman *et al.*, 2006).

We found that the inhibition of presynaptic N-type channels by MC4R activation occurs via G_s and in a voltage-independent manner. The voltage dependency is a critical property of G protein-coupled receptor-mediated VGCC inhibition (Lipscombe & Raingo, 2007). A voltage-dependent VGCC inhibition implies that the inhibition can be relieved when a train of action potentials reaches the synaptic terminal (Lipscombe & Raingo, 2007). The voltage-dependent G protein-coupled receptor-mediated mechanism is well described for $G_{i/o}$-coupled receptors and involves direct interaction between the channel and the Gβγ subunit of the G protein (Zamponi & Snutch, 1998; Ikeda & Dunlap, 1999; Raingo *et al.*, 2007). In contrast, voltage-independent inhibition depends on the Gα subunit of G proteins and involves diverse signaling pathways, including phosphorylation of the pore-forming subunit of VGCCs. Here, we found that MC4R-induced inhibition of N-type channels is fully voltage-independent, meaning that MC4R can induce a long-lasting inhibition at the synaptic level independent of the electrical neuronal activity. Also, we showed that RGS2, which is a general inhibitor of the GTPase activity of Gα proteins (Kehrl & Sinnarajah, 2002), as well as cholera toxin, which specifically impairs $G\alpha_s$ activity, occlude the MC4R-mediated inhibition. Thus, our results confirm that MC4R mostly signals via G_s activation (Gao *et al.*, 2003; Shinyama *et al.*, 2003; Tao, 2010). The current data agree with previous studies showing that other G_s-coupled receptors inhibit N-type channels in expression systems (Kisilevsky *et al.*, 2008) and in primary cultures of sympathetic (Zhu & Ikeda, 1994), hippocampal (Wu & Saggau, 1994; Gundlfinger *et al.*, 2007), neostratial (Surmeier *et al.*, 1995) and cerebellar (Dittman & Regehr, 1996) neurons. Moreover, the fact that MC4R failed to modulate P/Q-type channels is consistent with the notion that MC4R exclusively signals via G_s, and modulation of P/Q-type channels by this G-coupled protein has not been previously reported.

The molecular mechanisms underlying the neuronal effects of MC4R activation have been poorly studied. There are only a few studies describing the role of MC4R in hypothalamic synapses (Cone *et al.*, 2001; Daniels *et al.*, 2003; Chen *et al.*, 2012), whereas the mechanisms that mediate MC4R action at the amygdaloid complex remain obscure (Boghossian *et al.*, 2010). Here, we showed that MC4R activation specifically inhibits N-type currents in neurons from the amygdaloid complex, recapitulating our observations in the expression system. In most brain areas, presynaptic activity and short-term plasticity rely mainly on P/Q-type channel activity (Catterall *et al.*, 2013). In contrast, neurotransmitter release depends on both N-type and P/Q-type channel-mediated calcium entry in fewer brain areas, including the cerebellum and hippocampus (Poncer *et al.*, 1997; Ali & Nelson, 2006; Koch *et al.*, 2013). Thus, the presence of N-type channels offers a distinct property to certain synapses. Our current data, showing that the VGCC currents in embryonic amygdaloid complex neurons have a large ω conotoxin GVIA-sensitive component and a small ω agatoxin IVA-sensitive component, suggest that the MC4R modulation of N-type currents could be a relevant mechanism to control neurotransmitter release in the amygdala.

The MC4R activation increases neuronal activity in several brain areas including the amygdala (Benoit *et al.*, 2000) but the molecular mechanisms are not fully understood. Thus, we examined whether MC4R activation can modulate neurotransmission. As a large body of evidence indicates that MC4R can be presynaptically located (Cowley *et al.*, 1999; Fu & van den Pol, 2008; Wan *et al.*, 2008), we hypothesised that MC4R activation would involve presynaptic N-type channel inhibition and further GABA release reduction in the amygdala. In order to address this possibility, we used differentiated neuronal cultures of the amygdala as a model to evaluate the molecular properties of neurotransmission in a controlled manner. We found that MC4R activation inhibits GABAergic neurotransmission mainly via VGCC-dependent mechanisms. Indeed, MC4R activation did not modify GABA release stimulated by high-sucrose solution, which is known to release neurotransmitters in a VGCC-independent way. Moreover, we found a mild stimulatory effect on mIPSC amplitude that could be part of the postsynaptic actions of MC4R. However, we also tested whether excitatory postsynaptic currents are sensitive to MC4R activation and found that the MC4R agonist did not affect excitatory neurotransmission in our experimental conditions. The observed lack of effect of MC4R on glutamatergic neurotransmission could be due to glutamatergic terminals lacking MC4R or to a combination of the MC4R-induced stimulatory and inhibitory effect on glutamate release. An absence of the N-type calcium channel in excitatory terminals is a less likely explanation as previous reports showed that glutamate release is partially under the control of N-type currents in many brain nuclei (Huang *et al.*, 2003; Holderith *et al.*, 2012). The outcome of previous studies addressing the potential role of MC4R as a modulator of excitatory synapses is mixed. MC4R attenuates glutamatergic inputs at terminals of vagal afferent fibers innervating the nucleus of the solitary tract (Wan *et al.*, 2008). In contrast, MC4R activation enhances excitatory neurotransmitter release in hypothalamic ventromedial

nucleus neurons (Fu & van den Pol, 2008). Our data indicate that N-type channels could mediate an inhibitory presynaptic effect of MC4R at amygdala GABAergic neurons contributing to the global neuronal activation effect.

In order to explore whether our data have an impact in the intact adult amygdala, we mapped the distribution of c-Fos after MC4R activation or N-type channel blockade in amygdaloid nuclei. Our results not only confirmed previous studies showing that MC4R agonists increase c-Fos in the CeA (Benoit *et al.*, 2000) but also showed that this is significant in the BLA. When we assayed the blockade of N-type channels, we observed c-Fos expression induction in the CeA but not in the BLA. Thus, it is possible to hypothesise that the inhibition of these channels contributes to the mechanisms by which the MC4R agonist activates the CeA *in vivo*. In contrast, the MC4R-mediated increase of c-Fos in the BLA is possibly due to a postsynaptic effect unrelated to N-type current inhibition by MC4R. In order to activate c-Fos expression, the inhibition of N-type channels should occur in presynaptic terminals of GABAergic input neurons. GABAergic tone is an important regulator of several BLA and CeA functions (Sanders *et al.*, 1995; Pare *et al.*, 2004; Jovanovic & Ressler, 2010; Morozov *et al.*, 2011; Bienvenu *et al.*, 2012). A plausible explanation of why we found an excitatory effect of N-type channel block only in the CeA could be that this area has a more prominent GABAergic tone compared with the BLA (Sun & Cassell, 1993; Pare *et al.*, 2004) (Ehrlich *et al.*, 2009; Jovanovic & Ressler, 2010). The MC4R-containing GABA terminals innervating the CeA neurons could be provided by other appetite-related brain areas such as some hypothalamic nuclei (Haskell-Luevano *et al.*, 1999; Kishi *et al.*, 2003). However, as the CeA has a high density of local GABAergic neurons (Sun & Cassell, 1993; Pare *et al.*, 2004; Ehrlich *et al.*, 2009; Jovanovic & Ressler, 2010) and we showed that MC4R activation reduces GABA release in primary neuronal cultures obtained from the amygdaloid area, it is likely that MC4R is present at local GABAergic neuron terminals. Future studies performed in acute brain slices will be required to clarify the contribution of presynaptic MC4R to BLA neuron activation and to confirm that the N-type calcium channel-mediated inhibition of GABA release is an effector of the MC4R signaling that differentially activates CeA neurons *in vivo*. Moreover, experiments in intact tissue will also determine in which neurons those GABAergic terminals originate.

The amygdala, together with the hypothalamus, is the brain area with the highest MC4R expression levels (Kishi *et al.*, 2003; Liu *et al.*, 2003). The key role in food intake control of the MC4R signaling in the amygdala is highlighted by an elegant study showing that re-expression of MC4R exclusively in the PVN and amygdala is sufficient to restore food intake and prevent 60% of the obesity in MC4R-deficient mice (Balthasar *et al.*, 2005). The CeA, the area where our data suggest that N-type calcium channels could mediate MC4R effects, is probably one of the key brain targets mediating the anorexigenic actions of the melanocortin signaling. This is supported by observations that lesions of the amygdaloid complex in rats induce hyperphagia and obesity (King *et al.*, 1999). In addition, injections of MC4R agonists or antagonists in the CeA dose-dependently inhibited or increased food intake, respectively (Kask & Schioth, 2000).

In summary, we showed that MC4R activation exclusively inhibits N-type calcium channels and no other VGCCs. Based on *in vitro* and *in vivo* data, we postulate that this effect is important for the action of melanocortins in the CeA. Future studies will be needed to elucidate the physiological relevance of the MC4R-induced inhibition of N-type calcium channels in other brain areas. Hopefully, this information will be helpful to the development of MC4R-related pharmacological strategies for the treatment of hyperphagia.

Acknowledgements

We would like to thank Silvia S. Rodriguez for her excellent technical support, Dr Diane Lipscombe (Brown University) for the calcium channel clones, and Dr Mikhail Khvotchev and Dr Ege Kavalali for their invaluable help in constructing the MC4R-containing plasmid. This work was supported by grants from the National Agency of Scientific and Technological Promotion of Argentina (PICT2010-1954 and PICT2011-2142 to M.P. and PICT2010-1589 and PICT2011-1816 to J.R.). F.A. is a fellow of the Scientific Research Commission, Province of Buenos Aires, and E.J.L.S. and A.C. are fellows of CONICET.

Abbreviations

BLA, basolateral amygdala; CeA, central amygdala; ICV, intracerebroventricular; IPSC, inhibitory postsynaptic current; IR, immunoreactive; MC4R, melanocortin 4 receptor; mIPSC, miniature inhibitory postsynaptic current; MTII, melanotan II; PVN, paraventricular nucleus; RGS2, regulator G protein signaling 2; VGCC, voltage-gated calcium channel.

References

Ali, A.B. & Nelson, C. (2006) Distinct Ca^{2+} channels mediate transmitter release at excitatory synapses displaying different dynamic properties in rat neocortex. *Cereb. Cortex*, **16**, 386–393.

Balthasar, N., Dalgaard, L.T., Lee, C.E., Yu, J., Funahashi, H., Williams, T., Ferreira, M., Tang, V., McGovern, R.A., Kenny, C.D., Christiansen, L.M., Edelstein, E., Choi, B., Boss, O., Aschkenasi, C., Zhang, C.Y., Mountjoy, K., Kishi, T., Elmquist, J.K. & Lowell, B.B. (2005) Divergence of melanocortin pathways in the control of food intake and energy expenditure. *Cell*, **123**, 493–505.

Benoit, S.C., Schwartz, M.W., Lachey, J.L., Hagan, M.M., Rushing, P.A., Blake, K.A., Yagaloff, K.A., Kurylko, G., Franco, L., Danhoo, W. & Seeley, R.J. (2000) A novel selective melanocortin-4 receptor agonist reduces food intake in rats and mice without producing aversive consequences. *J. Neurosci.*, **20**, 3442–3448.

Bienvenu, T.C., Busti, D., Magill, P.J., Ferraguti, F. & Capogna, M. (2012) Cell-type-specific recruitment of amygdala interneurons to hippocampal theta rhythm and noxious stimuli in vivo. *Neuron*, **74**, 1059–1074.

Boghossian, S., Park, M. & York, D.A. (2010) Melanocortin activity in the amygdala controls appetite for dietary fat. *Am. J. Physiol.-Reg. I.*, **298**, R385–R393.

Cabral, A., Suescun, O., Zigman, J.M. & Perello, M. (2012) Ghrelin indirectly activates hypophysiotropic CRF neurons in rodents. *PLoS One*, **7**, e31462.

Catterall, W.A., Leal, K. & Nanou, E. (2013) Calcium channels and short-term synaptic plasticity. *J. Biol. Chem.*, **288**, 10742–10749.

Chen, M., Berger, A., Kablan, A., Zhang, J., Gavrilova, O. & Weinstein, L.S. (2012) Gsalpha deficiency in the paraventricular nucleus of the hypothalamus partially contributes to obesity associated with Gsalpha mutations. *Endocrinology*, **153**, 4256–4265.

Cone, R.D. (2005) Anatomy and regulation of the central melanocortin system. *Nat. Neurosci.*, **8**, 571–578.

Cone, R.D., Cowley, M.A., Butler, A.A., Fan, W., Marks, D.L. & Low, M.J. (2001) The arcuate nucleus as a conduit for diverse signals relevant to energy homeostasis. *Int. J. Obesity*, **25**(Suppl 5), S63–S67.

Cowley, M.A., Pronchuk, N., Fan, W., Dinulescu, D.M., Colmers, W.F. & Cone, R.D. (1999) Integration of NPY, AGRP, and melanocortin signals in the hypothalamic paraventricular nucleus: evidence of a cellular basis for the adipostat. *Neuron*, **24**, 155–163.

Currie, K.P. (2010) G protein modulation of CaV2 voltage-gated calcium channels. *Channels (Austin)*, **4**, 497–509.

Daniels, D., Patten, C.S., Roth, J.D., Yee, D.K. & Fluharty, S.J. (2003) Melanocortin receptor signaling through mitogen-activated protein kinase in vitro and in rat hypothalamus. *Brain Res.*, **986**, 1–11.

Dittman, J.S. & Regehr, W.G. (1996) Contributions of calcium-dependent and calcium-independent mechanisms to presynaptic inhibition at a cerebellar synapse. *J. Neurosci.*, **16**, 1623–1633.

Ehrlich, I., Humeau, Y., Grenier, F., Ciocchi, S., Herry, C. & Luthi, A. (2009) Amygdala inhibitory circuits and the control of fear memory. *Neuron*, **62**, 757–771.

Fan, W., Boston, B.A., Kesterson, R.A., Hruby, V.J. & Cone, R.D. (1997) Role of melanocortinergic neurons in feeding and the agouti obesity syndrome. *Nature*, **385**, 165–168.

Fehm, H.L., Smolnik, R., Kern, W., McGregor, G.P., Bickel, U. & Born, J. (2001) The melanocortin melanocyte-stimulating hormone/adrenocorticotropin(4-10) decreases body fat in humans. *J. Clin. Endocr. Metab.*, **86**, 1144–1148.

Fu, L.Y. & van den Pol, A.N. (2008) Agouti-related peptide and MC3/4 receptor agonists both inhibit excitatory hypothalamic ventromedial nucleus neurons. *J. Neurosci.*, **28**, 5433–5449.

Gantz, I., Miwa, H., Konda, Y., Shimoto, Y., Tashiro, T., Watson, S.J., DelValle, J. & Yamada, T. (1993) Molecular cloning, expression, and gene localization of a fourth melanocortin receptor. *J. Biol. Chem.*, **268**, 15174–15179.

Gao, Z., Lei, D., Welch, J., Le, K., Lin, J., Leng, S. & Duhl, D. (2003) Agonist-dependent internalization of the human melanocortin-4 receptors in human embryonic kidney 293 cells. *J. Pharmacol. Exp. Ther.*, **307**, 870–877.

Gelez, H., Poirier, S., Facchinetti, P., Allers, K.A., Wayman, C., Bernabe, J., Alexandre, L. & Giuliano, F. (2010) Neuroanatomical distribution of the melanocortin-4 receptors in male and female rodent brain. *J. Chem. Neuroanat.*, **40**, 310–324.

Ghamari-Langroudi, M., Srisai, D. & Cone, R.D. (2011) Multinodal regulation of the arcuate/paraventricular nucleus circuit by leptin. *Proc. Natl. Acad. Sci. USA*, **108**, 355–360.

Gundlfinger, A., Bischofberger, J., Johenning, F.W., Torvinen, M., Schmitz, D. & Breustedt, J. (2007) Adenosine modulates transmission at the hippocampal mossy fibre synapse via direct inhibition of presynaptic calcium channels. *J. Psychophysiol.*, **582**, 263–277.

Hagan, M.M., Rushing, P.A., Schwartz, M.W., Yagaloff, K.A., Burn, P., Woods, S.C. & Seeley, R.J. (1999) Role of the CNS melanocortin system in the response to overfeeding. *J. Neurosci.*, **19**, 2362–2367.

Han, J., Mark, M.D., Li, X., Xie, M., Waka, S., Rettig, J. & Herlitze, S. (2006) RGS2 determines short-term synaptic plasticity in hippocampal neurons by regulating Gi/o-mediated inhibition of presynaptic Ca^{2+} channels. *Neuron*, **51**, 575–586.

Haskell-Luevano, C., Chen, P., Li, C., Chang, K., Smith, M.S., Cameron, J.L. & Cone, R.D. (1999) Characterization of the neuroanatomical distribution of agouti-related protein immunoreactivity in the rhesus monkey and the rat. *Endocrinology*, **140**, 1408–1415.

Heximer, S.P., Watson, N., Linder, M.E., Blumer, K.J. & Hepler, J.R. (1997) RGS2/G0S8 is a selective inhibitor of Gqalpha function. *Proc. Natl. Acad. Sci. USA*, **94**, 14389–14393.

Holderith, N., Lorincz, A., Katona, G., Rozsa, B., Kulik, A., Watanabe, M. & Nusser, Z. (2012) Release probability of hippocampal glutamatergic terminals scales with the size of the active zone. *Nat. Neurosci.*, **15**, 988–997.

Huang, C.C., Chan, S.H. & Hsu, K.S. (2003) cGMP/protein kinase G-dependent potentiation of glutamatergic transmission induced by nitric oxide in immature rat rostral ventrolateral medulla neurons in vitro. *Mol. Pharmacol.*, **64**, 521–532.

Ikeda, S.R. & Dunlap, K. (1999) Voltage-dependent modulation of N-type calcium channels: role of G protein subunits. *Adv. Sec. Mess. Phosph.*, **33**, 131–151.

Ingi, T., Krumins, A.M., Chidiac, P., Brothers, G.M., Chung, S., Snow, B.E., Barnes, C.A., Lanahan, A.A., Siderovski, D.P., Ross, E.M., Gilman, A.G. & Worley, P.F. (1998) Dynamic regulation of RGS2 suggests a novel mechanism in G-protein signaling and neuronal plasticity. *J. Neurosci.*, **18**, 7178–7188.

Jovanovic, T. & Ressler, K.J. (2010) How the neurocircuitry and genetics of fear inhibition may inform our understanding of PTSD. *Am. J. Psychiat.*, **167**, 648–662.

Kask, A. & Schioth, H.B. (2000) Tonic inhibition of food intake during inactive phase is reversed by the injection of the melanocortin receptor antagonist into the paraventricular nucleus of the hypothalamus and central amygdala of the rat. *Brain Res.*, **887**, 460–464.

Kehrl, J.H. & Sinnarajah, S. (2002) RGS2: a multifunctional regulator of G-protein signaling. *Int. J. Biochem. Cell B.*, **34**, 432–438.

King, B.M., Rollins, B.L., Stines, S.G., Cassis, S.A., McGuire, H.B. & Lagarde, M.L. (1999) Sex differences in body weight gains following amygdaloid lesions in rats. *Am. J. Physiol.*, **277**, R975–R980.

Kishi, T., Aschkenasi, C.J., Lee, C.E., Mountjoy, K.G., Saper, C.B. & Elmquist, J.K. (2003) Expression of melanocortin 4 receptor mRNA in the central nervous system of the rat. *J. Comp. Neurol.*, **457**, 213–235.

Kisilevsky, A.E., Mulligan, S.J., Altier, C., Iftinca, M.C., Varela, D., Tai, C., Chen, L., Hameed, S., Hamid, J., Macvicar, B.A. & Zamponi, G.W. (2008) D1 receptors physically interact with N-type calcium channels to regulate channel distribution and dendritic calcium entry. *Neuron*, **58**, 557–570.

Koch, H., Zanella, S., Elsen, G.E., Smith, L., Doi, A., Garcia, A.J. 3rd, Wei, A.D., Xun, R., Kirsch, S., Gomez, C.M., Hevner, R.F. & Ramirez, J.M. (2013) Stable respiratory activity requires both P/Q-type and N-type voltage-gated calcium channels. *J. Neurosci.*, **33**, 3633–3645.

Lee, S.C., Choi, S., Lee, T., Kim, H.L., Chin, H. & Shin, H.S. (2002) Molecular basis of R-type calcium channels in central amygdala neurons of the mouse. *Proc. Natl. Acad. Sci. USA*, **99**, 3276–3281.

Lipscombe, D. & Raingo, J. (2007) Alternative splicing matters: N-type calcium channels in nociceptors. *Channels (Austin)*, **1**, 225–227.

Liu, H., Kishi, T., Roseberry, A.G., Cai, X., Lee, C.E., Montez, J.M., Friedman, J.M. & Elmquist, J.K. (2003) Transgenic mice expressing green fluorescent protein under the control of the melanocortin-4 receptor promoter. *J. Neurosci.*, **23**, 7143–7154.

Maximov, A., Sudhof, T.C. & Bezprozvanny, I. (1999) Association of neuronal calcium channels with modular adaptor proteins. *J. Biol. Chem.*, **274**, 24453–24456.

Missler, M., Zhang, W., Rohlmann, A., Kattenstroth, G., Hammer, R.E., Gottmann, K. & Sudhof, T.C. (2003) Alpha-neurexins couple Ca^{2+} channels to synaptic vesicle exocytosis. *Nature*, **423**, 939–948.

Morozov, A., Sukato, D. & Ito, W. (2011) Selective suppression of plasticity in amygdala inputs from temporal association cortex by the external capsule. *J. Neurosci.*, **31**, 339–345.

Mountjoy, K.G., Mortrud, M.T., Low, M.J., Simerly, R.B. & Cone, R.D. (1994) Localization of the melanocortin-4 receptor (MC4-R) in neuroendocrine and autonomic control circuits in the brain. *Mol. Endocrinol.*, **8**, 1298–1308.

Newman, E.A., Chai, B.X., Zhang, W., Li, J.Y., Ammori, J.B. & Mulholland, M.W. (2006) Activation of the melanocortin-4 receptor mobilizes intracellular free calcium in immortalized hypothalamic neurons. *J. Surg. Res.*, **132**, 201–207.

Pare, D., Quirk, G.J. & Ledoux, J.E. (2004) New vistas on amygdala networks in conditioned fear. *J. Neurophysiol.*, **92**, 1–9.

Paxinos, G. & Franklin, K. (2001) *The Mouse Brain*. 2nd Edn. Academic Press, San Diego, CA.

Poncer, J.C., McKinney, R.A., Gahwiler, B.H. & Thompson, S.M. (1997) Either N- or P-type calcium channels mediate GABA release at distinct hippocampal inhibitory synapses. *Neuron*, **18**, 463–472.

Raingo, J., Castiglioni, A.J. & Lipscombe, D. (2007) Alternative splicing controls G protein-dependent inhibition of N-type calcium channels in nociceptors. *Nat. Neurosci.*, **10**, 285–292.

Raingo, J., Khvotchev, M., Liu, P., Darios, F., Li, Y.C., Ramirez, D.M., Adachi, M., Lemieux, P., Toth, K., Davletov, B. & Kavalali, E.T. (2012) VAMP4 directs synaptic vesicles to a pool that selectively maintains asynchronous neurotransmission. *Nat. Neurosci.*, **15**, 738–745.

Roy, A.A., Baragli, A., Bernstein, L.S., Hepler, J.R., Hebert, T.E. & Chidiac, P. (2006a) RGS2 interacts with Gs and adenylyl cyclase in living cells. *Cell. Signal.*, **18**, 336–348.

Roy, A.A., Nunn, C., Ming, H., Zou, M.X., Penninger, J., Kirshenbaum, L.A., Dixon, S.J. & Chidiac, P. (2006b) Up-regulation of endogenous RGS2 mediates cross-desensitization between Gs and Gq signaling in osteoblasts. *J. Biol. Chem.*, **281**, 32684–32693.

Sah, P., Faber, E.S., Lopez De Armentia, M. & Power, J. (2003) The amygdaloid complex: anatomy and physiology. *Physiol. Rev.*, **83**, 803–834.

Sanders, S.K., Morzorati, S.L. & Shekhar, A. (1995) Priming of experimental anxiety by repeated subthreshold GABA blockade in the rat amygdala. *Brain Res.*, **699**, 250–259.

Schioth, H.B. (2006) G protein-coupled receptors in regulation of body weight. *CNS Neurol. Disord.-Dr.*, **5**, 241–249.

Shinyama, H., Masuzaki, H., Fang, H. & Flier, J.S. (2003) Regulation of melanocortin-4 receptor signaling: agonist-mediated desensitization and internalization. *Endocrinology*, **144**, 1301–1314.

Sun, N. & Cassell, M.D. (1993) Intrinsic GABAergic neurons in the rat central extended amygdala. *J. Comp. Neurol.*, **330**, 381–404.

Surmeier, D.J., Bargas, J., Hemmings, H.C. Jr., Nairn, A.C. & Greengard, P. (1995) Modulation of calcium currents by a D1 dopaminergic protein kinase/phosphatase cascade in rat neostriatal neurons. *Neuron*, **14**, 385–397.

Swanson, L.W. & Petrovich, G.D. (1998) What is the amygdala? *Trends Neurosci.*, **21**, 323–331.

Tao, Y.X. (2010) The melanocortin-4 receptor: physiology, pharmacology, and pathophysiology. *Endocr. Rev.*, **31**, 506–543.

Tedford, H.W. & Zamponi, G.W. (2006) Direct G protein modulation of Cav2 calcium channels. *Pharmacol. Rev.*, **58**, 837–862.
Thaler, C., Gray, A.C. & Lipscombe, D. (2004) Cumulative inactivation of N-type CaV2.2 calcium channels modified by alternative splicing. *Proc. Natl. Acad. Sci. USA*, **101**, 5675–5679.
Thiele, T.E., van Dijk, G., Yagaloff, K.A., Fisher, S.L., Schwartz, M., Burn, P. & Seeley, R.J. (1998) Central infusion of melanocortin agonist MTII in rats: assessment of c-Fos expression and taste aversion. *Am. J. Physiol.*, **274**, R248–R254.
Wan, S., Browning, K.N., Coleman, F.H., Sutton, G., Zheng, H., Butler, A., Berthoud, H.R. & Travagli, R.A. (2008) Presynaptic melanocortin-4 receptors on vagal afferent fibers modulate the excitability of rat nucleus tractus solitarius neurons. *J. Neurosci.*, **28**, 4957–4966.
Wu, L.G. & Saggau, P. (1994) Adenosine inhibits evoked synaptic transmission primarily by reducing presynaptic calcium influx in area CA1 of hippocampus. *Neuron*, **12**, 1139–1148.
Zamponi, G.W. & Snutch, T.P. (1998) Modulation of voltage-dependent calcium channels by G proteins. *Curr. Opin. Neurobiol.*, **8**, 351–356.
Zhu, Y. & Ikeda, S.R. (1994) VIP inhibits N-type Ca^{2+} channels of sympathetic neurons via a pertussis toxin-insensitive but cholera toxin-sensitive pathway. *Neuron*, **13**, 657–669.